$k \cdot p$ Perturbation and Energy Bands of Semiconductors

Chihiro Hamaguchi

Professor Emeritus of Osaka University

June 4, 2013

Outline

1. Introduction to $\boldsymbol{k} \cdot \boldsymbol{p}$ perturbation and energy band calculations
   - 1.1 Bloch function
   - 1.2 $\boldsymbol{k} \cdot \boldsymbol{p}$ Hamiltonian
   - 1.3 Empty lattice bands and pseudopotential method
   - 1.4 $\boldsymbol{k} \cdot \boldsymbol{p}$ parameters and energy bands

2. Valence band analysis by $\boldsymbol{k} \cdot \boldsymbol{p}$ perturbation
   - 2.1 Second order $\boldsymbol{k} \cdot \boldsymbol{p}$ perturbation
   - 2.2 Spin-orbit interaction
   - 2.3 Dresselhaus Hamiltonian
   - 2.4 Valence bands dispersion and eigen states
   - 2.5 Luttinger Hamiltonian

1.1 Bloch function

The non-relativistic Schrödinger equation for one-electron system:

$$\left[-\frac{\hbar^2}{2m}\nabla^2 + V(\boldsymbol{r})\right]\Psi(\boldsymbol{r}) = \mathcal{E}\Psi(\boldsymbol{r}) \tag{1}$$

The solution for a periodic potential $V(\boldsymbol{r})$ is given by Bloch function

$$\Psi(\boldsymbol{r}) = \mathrm{e}^{\mathrm{i}\boldsymbol{k}\cdot\boldsymbol{r}} u_{n,\boldsymbol{k}}(\boldsymbol{r}) \tag{2}$$

where $u_{n,\boldsymbol{k}}$ is a function with the lattice periodicity for band index n.

$$\boldsymbol{k} = \frac{2\pi}{L}(n_x, n_y, n_z) \quad n_x, n_y, n_z = 0, \pm 1, \pm 1, \pm 3, \cdots$$

1.2(1) $\boldsymbol{k}\cdot\boldsymbol{p}$ Hamiltonian

Differentiation of Bloch function :

$$\begin{aligned}\nabla\Psi(\boldsymbol{r}) &= \mathrm{i}\boldsymbol{k}\Psi(\boldsymbol{r}) + \mathrm{e}^{\mathrm{i}\boldsymbol{k}\cdot\boldsymbol{r}}\nabla u_{n,\boldsymbol{k}}(\boldsymbol{r}) \qquad (3)\\ \nabla^2\Psi(\boldsymbol{r}) &= -k^2\Psi(\boldsymbol{r}) + 2\mathrm{i}\boldsymbol{k}\mathrm{e}^{\mathrm{i}\boldsymbol{k}\cdot\boldsymbol{r}}\nabla u_{n,\boldsymbol{k}}(\boldsymbol{r}) + \mathrm{e}^{\mathrm{i}\boldsymbol{k}\cdot\boldsymbol{r}}\nabla^2 u_{n,\boldsymbol{k}}(\boldsymbol{r})\\ &= \mathrm{e}^{\mathrm{i}\boldsymbol{k}\cdot\boldsymbol{r}}(-k^2 + 2\mathrm{i}\boldsymbol{k}\cdot\nabla + \nabla^2)u_{n,\boldsymbol{k}}(\boldsymbol{r}) \qquad (4)\end{aligned}$$

Putting the above relations into (1) we obtain

$$\left[-\frac{\hbar^2}{2m}\nabla^2 + V(\boldsymbol{r}) + \frac{\hbar^2}{2m}k^2 - \mathrm{i}\frac{\hbar^2}{m}(\boldsymbol{k}\cdot\nabla)\right] u_{n,\boldsymbol{k}}(\boldsymbol{r}) = \mathcal{E}_n(\boldsymbol{k})u_{n,\boldsymbol{k}}(\boldsymbol{r}) \qquad (5)$$

1.2(2) $\boldsymbol{k} \cdot \boldsymbol{p}$ Hamiltonian

Above equation is rewritten by using the relation $\boldsymbol{p} = -\mathrm{i}\hbar\nabla$ as follows

$$\left[H_0 + H_{kp} + \frac{\hbar^2 k^2}{2m}\right] u_{n,\boldsymbol{k}}(\boldsymbol{r}) = \mathcal{E}_n(\boldsymbol{k}) u_{n,\boldsymbol{k}}(\boldsymbol{r}) \tag{6}$$

$$H_0 = -\frac{\hbar^2}{2m}\nabla^2 + V(\boldsymbol{r}) \tag{7}$$

$$H_{kp} = \frac{\hbar}{m}\boldsymbol{k} \cdot \boldsymbol{p} \tag{8}$$

Since $\hbar^2 k^2/2m$ has no operator (c-number), Schrödinger equation is solved by treating H_{kp} as a perturbing term.

1.2(3) Atomic units

We introduce atomic units:
Bohr radius: $a_{\mathrm{B}} = 4\pi\epsilon_0\hbar^2/(me^2) \simeq 0.529$ [A]
Rydberg constant: $[\mathrm{Ry}] = (\hbar^2/2m)/a_{\mathrm{B}}^2 = me^4/(8\epsilon^2 h^3 c)$
$\simeq 13.6$ [eV]

$$\boldsymbol{k}\,(\text{in [a.u]}) = a_{\mathrm{B}}\boldsymbol{k}\,, \qquad \boldsymbol{p}\,(\text{in [a.u]}) = \frac{a_{\mathrm{B}}}{\hbar}\boldsymbol{p} = -\mathrm{i}a_{\mathrm{B}}\nabla\,, \tag{9}$$

and then the $\boldsymbol{k}\cdot\boldsymbol{p}$ operator in atomic units is rewritten as

$$\frac{\hbar}{m}\boldsymbol{k}\cdot\boldsymbol{p} = \frac{\hbar^2}{2m}\left(\frac{1}{a_{\mathrm{B}}}\right)^2 2a_{\mathrm{B}}\boldsymbol{k}\cdot\frac{a_{\mathrm{B}}}{\hbar}\boldsymbol{p} = \mathrm{Ry}\cdot(2\boldsymbol{k}\cdot\boldsymbol{p}) \tag{10}$$

1.2(4) $\boldsymbol{k} \cdot \boldsymbol{p}$ Hamiltonian in atomic units

Then the Schrödinger equation equation(6) or the $\boldsymbol{k} \cdot \boldsymbol{p}$ Hamiltonian is rewritten as

$$H_0 + \frac{\hbar}{m}\boldsymbol{k} \cdot \boldsymbol{p} + \frac{\hbar^2 k^2}{2m} = -\nabla^2 + 2\boldsymbol{k} \cdot \boldsymbol{p} + k^2 \,. \qquad (11)$$

Once we know the eigen values at $\boldsymbol{k} = 0$, equation(11) is solved by assuming the term $2\boldsymbol{k} \cdot \boldsymbol{p}$ as the perturbation term.
In the following we estimate the energy eigen values at $\boldsymbol{k} = 0$, and estimate the matrix elements of $2\boldsymbol{k} \cdot \boldsymbol{p}$ for 15 eigen states.

1.3(1) Energy eigen states at $\boldsymbol{k} = 0$

When $\boldsymbol{k} = 0$, equation (5) or (6) reduces to

$$\left[-\frac{\hbar^2}{2m}\nabla^2 + V(\boldsymbol{r})\right] u_n(\boldsymbol{r}) = \mathcal{E}_n u_n(\boldsymbol{r}) \tag{12}$$

This equation gives the energies at $\boldsymbol{k} = 0$ (Γ point). Once we obtain the energies at the Γ point, and then the energy eigen values in "specific directions" of the Brillouin zone are calculated assuming the H_{kp} as the perturbing term. However, the solutions of the above equation is not easily obtained. One of the easiest method to estimate the energy eigen values at $\boldsymbol{k} = 0$ to use "empirical pseudopotential method".

1.3(2) Reciprocal lattice vectors of fcc crystals–1

$\boldsymbol{a} = (a/2)(\boldsymbol{e}_x + \boldsymbol{e}_y)$, $\boldsymbol{b} = (a/2)(\boldsymbol{e}_y + \boldsymbol{e}_z)$, $\boldsymbol{c} = (a/2)(\boldsymbol{e}_z + \boldsymbol{e}_x)$

$$\begin{aligned} \boldsymbol{a}^* &= \frac{\boldsymbol{b} \times \boldsymbol{c}}{\boldsymbol{a} \cdot (\boldsymbol{b} \times \boldsymbol{c})} = \left(\frac{a}{2}\right)^2 \frac{(\boldsymbol{e}_y + \boldsymbol{e}_z) \times (\boldsymbol{e}_z + \boldsymbol{e}_x)}{v} \\ &= \frac{1}{a}(\boldsymbol{e}_x + \boldsymbol{e}_y - \boldsymbol{e}_z) \end{aligned}$$

Similarly $\boldsymbol{b}^*$ and $\boldsymbol{c}^*$ are calculated, and the reciprocal lattice vectors are defined as

$$\begin{aligned} \boldsymbol{G} &= 2\pi[n_1\boldsymbol{a}^* + n_2\boldsymbol{b}^* + n_3\boldsymbol{c}^*] \\ &= \frac{2\pi}{a}\left[(n_1 - n_2 + n_3)\boldsymbol{e}_x + (n_1 + n_2 - n_3)\boldsymbol{e}_y \right. \\ &\qquad \left. +(-n_1 + n_2 + n_3)\boldsymbol{e}_z\right], \\ &\quad n_1, n_2, n_3 = 0, \pm 1, \pm 2, \pm 3, \cdots\cdots \end{aligned}$$

1.3(3) Reciprocal lattice vectors for fcc crystals–2

The smaller reciprocal lattice vectors are

$\boldsymbol{G}$	vector components	dgn	representations
$\boldsymbol{G}_0$	$= (2\pi/a)(0,0,0)$	1	Γ_1^l
$\boldsymbol{G}_3$	$= (2\pi/a)(\pm1,\pm1,\pm1)$	8	$\Gamma_{25'}^l + \Gamma_{15} + \Gamma_{2'}^l + \Gamma_1^u$
$\boldsymbol{G}_4$	$= (2\pi/a)(\pm2,0,0)$	6	$\Gamma_{25'}^u + \Gamma_{12'} + \Gamma_{2'}^u$
$\boldsymbol{G}_8$	$= (2\pi/a)(\pm2,\pm2,0)$	12	$\Gamma_1 + \Gamma_{12} + 2\Gamma_{15} + \Gamma_{25'}$
$\boldsymbol{G}_{11}$	$= (2\pi/a)(\pm3,\pm1,\pm1)$	24	$\Gamma_1 + \Gamma_{12} + \Gamma_2 + \Gamma_{12'}$ $\Gamma_{15'} + \Gamma_{25} + 2\Gamma_{25'} + 2\Gamma_{15}$

where “dgn” means “degeneracy”.

1.4(1) Empty lattice bands–1

Empty lattice bands in [100] direction:

$$
\begin{aligned}
\boldsymbol{G}_0: \quad \mathcal{E} &= k_x^2\,, \\
\boldsymbol{G}_3: \quad \mathcal{E} &= (k_x \pm 1)^2 + (\pm 1)^2 + (\pm 1)^2 \\
&= \begin{cases} (k_x - 1)^2 + 2 & \text{(4-fold degeneracy)} \\ (k_x + 1)^2 + 2 & \text{(4-fold degeneracy)} \end{cases}, \\
\boldsymbol{G}_4: \quad \mathcal{E} &= \begin{cases} k_x^2 + 4 & \text{(4-fold degeneracy)} \\ (k_x - 2)^2 & \text{(single state)} \\ (k_x + 2)^2 & \text{(single state)} \end{cases}
\end{aligned}
$$

where the energy is measured in the units $\hbar^2(2\pi/a)^2/2m$ and the wave vector $\boldsymbol{k}$ in the units $2\pi/a$. When we plot these relations, we obtain the curves shown in the following figure.

1.4(2) Empty lattice bands–2

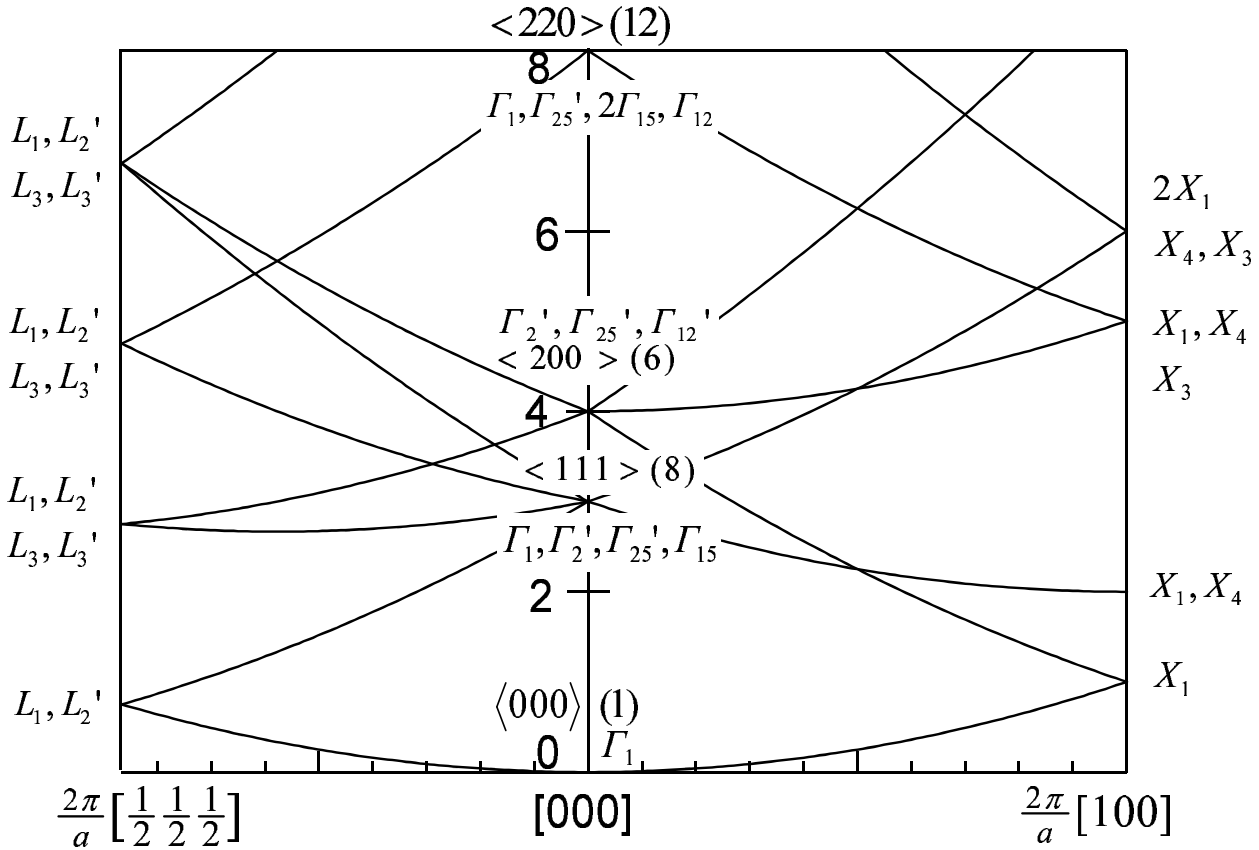

Empty lattice bands of fcc crystals, where the number in the parentheses is the degeneracy and the representations are shown.

1.4(3) Pseudopotential method

The energy eigen values are evaluated using the pseudopotentials (see C. Hamaguchi: "*Basic Semiconductor Physics*", (Springer, 2010)). An arbitrary function which satisfies the orthogonality with respect to the core states of a crystal is given by

$$|\Psi(\boldsymbol{k},\boldsymbol{r})\rangle = |\chi_n(\boldsymbol{k},\boldsymbol{r})\rangle - \sum_j \langle\varphi_j|\chi_n\rangle|\varphi_j\rangle\,. \tag{13}$$

Then Schrödinger equation is rewritten as

$$H|\chi_n\rangle + \sum_j [\mathcal{E}_n(\boldsymbol{k}) - \mathcal{E}_j]|\varphi_j\rangle\langle\varphi_j|\chi_n\rangle = \mathcal{E}_n(\boldsymbol{k})|\chi_n\rangle \tag{14}$$

$$[H + V_{\rm p}]|\chi_n\rangle = \mathcal{E}_n(\boldsymbol{k})|\chi_n\rangle \tag{15}$$

$$V_{\rm p} = \sum_j [\mathcal{E}_n(\boldsymbol{k}) - \mathcal{E}_j]|\varphi_j\rangle\langle\varphi_j| \tag{16}$$

1.4(4) Pseudopotential Hamiltonian

Since $\mathcal{E}_n(\boldsymbol{k}) > \mathcal{E}_j$, and thus we find that $V_\mathrm{p} > 0$. Then we may rewrite (15) as

$$[H_0 + V(\boldsymbol{r}) + V_\mathrm{p}(\boldsymbol{r})]|\chi_n\rangle = \mathcal{E}_n(\boldsymbol{k})|\chi_n\rangle \tag{17}$$

$$[H_0 + V_\mathrm{ps}(\boldsymbol{r})]|\chi_n\rangle = \mathcal{E}_n(\boldsymbol{k})|\chi_n\rangle \tag{18}$$

$$V_\mathrm{ps} = V(\boldsymbol{r}) + V_\mathrm{p}(\boldsymbol{r}) \tag{19}$$

Since $V_\mathrm{p} > 0$ and $V(\boldsymbol{r}) < 0$, it may be possible to make V_ps small enough. The new potential $V_\mathrm{ps}(\boldsymbol{r})$, called **pseudopotential**, which is also periodic and is expanded in the Fourier series

$$V_\mathrm{ps}(\boldsymbol{r}) = \sum_j V_\mathrm{ps}(\boldsymbol{G}_j)\mathrm{e}^{-\mathrm{i}\boldsymbol{G}_j\cdot\boldsymbol{r}} \tag{20}$$

where the Fourier coefficients $V_\mathrm{ps}(\boldsymbol{G}_j)$ are given by

$$V_\mathrm{ps}(\boldsymbol{G}_j) = \frac{1}{\sqrt{\Omega}}\int_\Omega V_\mathrm{ps}(\boldsymbol{r})\mathrm{e}^{\mathrm{i}\boldsymbol{G}_j\cdot\boldsymbol{r}}\mathrm{d}^3\boldsymbol{r} \tag{21}$$

1.4(5) Fourier expansion of Bloch function and pseudopotentials

Crystal potential $V(\boldsymbol{r})$ and Bloch function $u_{n,\boldsymbol{k}}(\boldsymbol{r})$ are periodic with the lattice constant, and thus are expanded by Fourier series.

$$u_{\boldsymbol{k}}(\boldsymbol{r}) \to \frac{1}{\sqrt{\Omega}} \mathrm{e}^{\mathrm{i}(\boldsymbol{k}+\boldsymbol{G}_i)\cdot\boldsymbol{r}} = |(\boldsymbol{k}+\boldsymbol{G}_i)\rangle$$

$$V_{ps}(\boldsymbol{r}) = \sum_l V_{ps}(\boldsymbol{G}_l)\mathrm{e}^{-\mathrm{i}\boldsymbol{G}_l\cdot\boldsymbol{r}}$$

Then we obtain

$$\left[-\nabla^2 + \sum_l V_{ps}(\boldsymbol{G}_l)\mathrm{e}^{-\mathrm{i}\boldsymbol{G}_l\cdot\boldsymbol{r}}\right] |(\boldsymbol{k}+\boldsymbol{G}_i)\rangle = \mathcal{E}_n |(\boldsymbol{k}+\boldsymbol{G}_i)\rangle \,,$$

$$|(\boldsymbol{k}+\boldsymbol{G}_i)\rangle = \frac{1}{\sqrt{\Omega}} \mathrm{e}^{\mathrm{i}(\boldsymbol{k}+\boldsymbol{G}_i)\cdot\boldsymbol{r}}$$

Putting $\boldsymbol{k} = 0$, we obtain the eigen energies at the Γ point.

1.4(6) Secular equation of pseudopotential Hamiltonian

Multiplying

$$\langle(\boldsymbol{k}+\boldsymbol{G}_j)| = \frac{1}{\sqrt{\Omega}}\mathrm{e}^{-\mathrm{i}(\boldsymbol{k}+\boldsymbol{G}_j)\cdot\boldsymbol{r}}$$

from the left hand side and using the relation

$$\langle \boldsymbol{G}_J|\boldsymbol{G}_i\rangle = \frac{1}{\Omega}\int_\Omega \mathrm{e}^{\mathrm{i}(\boldsymbol{G}_i-\boldsymbol{G}_j)\cdot\boldsymbol{r}} = \delta_{\boldsymbol{G}_i,\boldsymbol{G}_j}$$

then the secular equation results in

$$\left[(\boldsymbol{k}+\boldsymbol{G}_j)^2\delta_{\boldsymbol{G}_i,\boldsymbol{G}_j} + V_{ps}(\boldsymbol{G}_i-\boldsymbol{G}_j) - \mathcal{E}(\boldsymbol{k})\delta_{\boldsymbol{G}_i,\boldsymbol{G}_j}\right] = 0$$

We will show in the following only three pseudopotentials $V_{ps}(|\boldsymbol{G}|) = V^S(G_33)$, $V^S(G_8)$ and $V^S(G_{11})$ are enough to calculate the energy bands of diamond structure.

1.4(7) Pseudopotential components

Since a crystal with fcc structure has two atoms (A and B) in the unit cell, we use the average potential

$$V_{ps}(\boldsymbol{G}_j) = \frac{1}{2}\sum_j \left[V_A(\boldsymbol{G}_j)\mathrm{e}^{\mathrm{i}\boldsymbol{G}_j\cdot\boldsymbol{\tau}} + V_B(\boldsymbol{G}_j)\mathrm{e}^{-\mathrm{i}\boldsymbol{G}_j\cdot\boldsymbol{\tau}}\right]\mathrm{e}^{-\mathrm{i}\boldsymbol{G}\cdot\boldsymbol{r}} \quad (22)$$

$$= \sum_j \left[V^S(\boldsymbol{G}_j)\cos(\boldsymbol{G}\cdot\boldsymbol{\tau}) + \mathrm{i}V^A(\boldsymbol{G}_j)\sin(\boldsymbol{G}\cdot\boldsymbol{\tau})\right] \times \mathrm{e}^{-\mathrm{i}\boldsymbol{G}\cdot\boldsymbol{r}} \quad (23)$$

$$V^S(\boldsymbol{G}_j) = \frac{1}{2}[V_A(\boldsymbol{G}_j) + V_B(\boldsymbol{G}_j)] \quad (24)$$

$$V^A(\boldsymbol{G}_j) = \frac{1}{2}[V_A(\boldsymbol{G}_j) - V_B(\boldsymbol{G}_j)] \quad (25)$$

For diamond structures: $V^A = 0$
and for zinc blende types: $V^A \neq 0$

1.4(8) Non-vanishing pseudopotential form factors

For a diamond crystal we find

$$V^{\mathrm{S}}(G_j)\cos\left(\boldsymbol{G}_j\cdot\boldsymbol{\tau}\right)=V^{\mathrm{S}}(\boldsymbol{G}_j)\cos\left(\frac{a}{8}\left[G_{jx}+G_{jy}+G_{jz}\right]\right)$$

Using the reciprocal lattice vectors of fcc crystals we find:

$$V^{\mathrm{S}}(\boldsymbol{G}_0)\cos\left(\boldsymbol{G}_0\cdot\boldsymbol{\tau}\right)=V^{\mathrm{S}}(\boldsymbol{G}_0)$$

$$V^{\mathrm{S}}(\boldsymbol{G}_3)\cos\left(\boldsymbol{G}_3\cdot\boldsymbol{\tau}\right)=V^{\mathrm{S}}(\boldsymbol{G}_3)\cos\left(\frac{\pi}{4}\left[\pm1\pm1\pm1\right]\right)\neq0$$

$$V^{\mathrm{S}}(\boldsymbol{G}_4)\cos\left(\boldsymbol{G}_4\cdot\boldsymbol{\tau}\right)=V^{\mathrm{S}}(\boldsymbol{G}_4)\cos\left(\frac{\pi}{4}\left[\pm2\right]\right)=0$$

$$V^{\mathrm{S}}(\boldsymbol{G}_8)\cos\left(\boldsymbol{G}_8\cdot\boldsymbol{\tau}\right)=V^{\mathrm{S}}(\boldsymbol{G}_8)\cos\left(\frac{\pi}{4}\left[\pm2\pm2\right]\right)\neq0$$

$$V^{\mathrm{S}}(\boldsymbol{G}_{11})\cos\left(\boldsymbol{G}_{11}\cdot\boldsymbol{\tau}\right)=V^{\mathrm{S}}(\boldsymbol{G}_{11})\cos\left(\frac{\pi}{4}\left[\pm3\pm1\pm1\right]\right)\neq0$$

Non-vanishing coefficients are therefore $V_{ps}(|\boldsymbol{G}|)=V^S(G_3)$, $V^S(G_8)$ and $V^S(G_{11})$, where we put $V^S(G_0)=0$.

1.4(9) Pseudopotential form factors

Table: Pseudopotentials for several semiconductors in units of Rydberg [Ry] and lattice constants a in [A](from M. L. Cohen and T. K. Bergstresser:Phys. Rev.**141** (1966) 789

	a[A]	V_3^S	V_8^S	V_{11}^S	V_3^A	V_4^A	V_{11}^A
Si	5.43	-0.21	$+0.04$	$+0.08$	0	0	0
Ge	5.66	-0.23	$+0.01$	$+0.06$	0	0	0
GaP	5.44	-0.22	$+0.03$	$+0.07$	$+0.12$	$+0.07$	$+0.02$
GaAs	5.64	-0.23	$+0.01$	$+0.06$	$+0.07$	$+0.05$	$+0.01$
AlSb	6.13	-0.21	$+0.02$	$+0.06$	$+0.06$	$+0.04$	$+0.02$
InP	5.86	-0.23	$+0.01$	$+0.06$	$+0.07$	$+0.05$	$+0.01$
InAs	6.04	-0.22	0.00	$+0.05$	$+0.08$	$+0.05$	$+0.03$
InSb	6.48	-0.20	0.00	$+0.04$	$+0.06$	$+0.05$	$+0.01$

1.4(10) Energy bands calculated by EPM

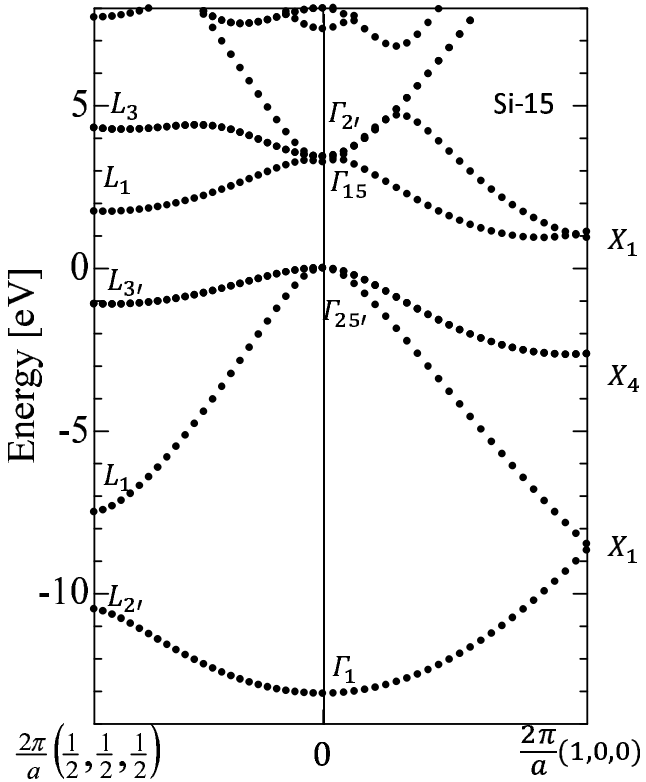

Figure: Energy band structure of Si calculated by 15 plane waves

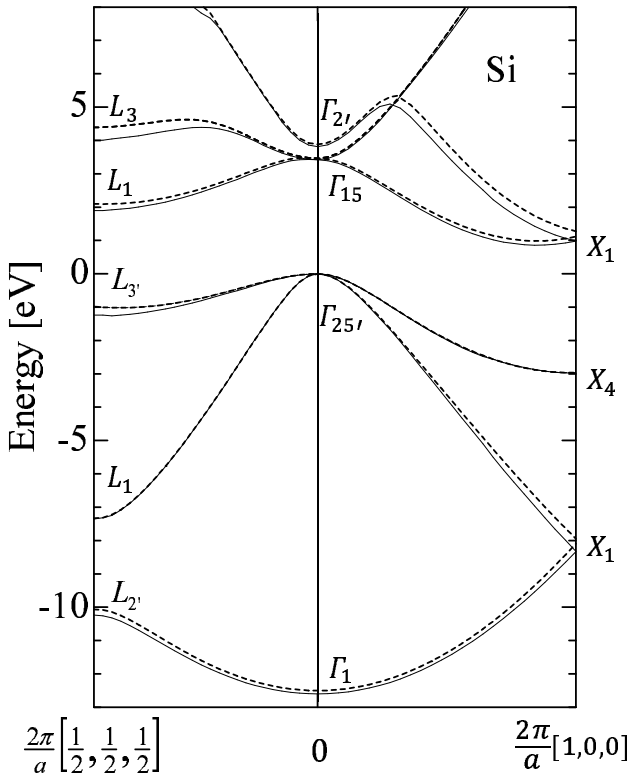

Figure: Energy band structure calculated by 27 (dotted) and 113 (solids) plane waves

1.4(11) Formulation of non-vanishing $\boldsymbol{k} \cdot \boldsymbol{p}$ parameters

Matrix elements of 15×15 $\boldsymbol{k} \cdot \boldsymbol{p}$ perturbation are evaluated as follows. For example, the basis functions of $\Gamma_{25'}$ are $|X\rangle = |yz\rangle$, $|Y\rangle = |zx\rangle$, and $|Z\rangle = |xy\rangle$, and $\Gamma_{2'} = |xyz\rangle$. Therefore we find

$$2\mathrm{i}\langle \Gamma^l_{25'} | p_x | \Gamma^l_{2'} \rangle = 2\mathrm{i}\langle X | p_x | xyz \rangle = P$$

where the superscript l (u) means lower (upper) states and Γ^l_{25} and $\Gamma^u_{25'}$ arise from the plane waves [111] and [200], respectively.
All the non-zero matrix elements of 15 $\boldsymbol{k} \cdot \boldsymbol{p}$ perturbation term are summarized in the next view graph.

1.4(12) Momentum matrix elements for $\boldsymbol{k}\cdot\boldsymbol{p}$

$$
\begin{aligned}
P &= 2\mathrm{i}\langle\Gamma^l_{25'}|\boldsymbol{p}|\Gamma^l_{2'}\rangle \\
Q &= 2\mathrm{i}\langle\Gamma^l_{25'}|\boldsymbol{p}|\Gamma_{15}\rangle \\
R &= 2\mathrm{i}\langle\Gamma^l_{25'}|\boldsymbol{p}|\Gamma_{12'}\rangle \\
P'' &= 2\mathrm{i}\langle\Gamma^l_{25'}|\boldsymbol{p}|\Gamma^u_{2'}\rangle, \\
P' &= 2\mathrm{i}\langle\Gamma^u_{25'}|\boldsymbol{p}|\Gamma^l_{2'}\rangle \\
Q' &= 2\mathrm{i}\langle\Gamma^u_{25'}|\boldsymbol{p}|\Gamma_{15}\rangle \\
R' &= 2\mathrm{i}\langle\Gamma^u_{25'}|\boldsymbol{p}|\Gamma_{12'}\rangle \\
P''' &= 2\mathrm{i}\langle\Gamma^u_{25'}|\boldsymbol{p}|\Gamma^u_{2'}\rangle \\
T &= 2\mathrm{i}\langle\Gamma^u_{1}|\boldsymbol{p}|\Gamma_{15}\rangle \\
T' &= 2\mathrm{i}\langle\Gamma^l_{1}|\boldsymbol{p}|\Gamma_{15}\rangle
\end{aligned}
$$

See the basis functions listed in the next Table. The matrix elements and eigen states are evaluated by solving 15×15 empirical pseudopotential theory. Then, these values are adjusted for $15\times15\,\boldsymbol{k}\cdot\boldsymbol{p}$ Hamiltonian matrix.

1.4 (13) Basis functions for group theoretical representations

Basis function of irreducible representation of O_h group at Γ point

representation	degeneracy	basis functions
Γ_1	1	1
Γ_2	1	$x^4(y^2-z^2)+y^4(z^2-x^2)+z^4(x^2-y^2)$
Γ_{12}	2	$z^2-\frac{1}{2}(x^2+y^2),\ (x^2-y^2)$
$\Gamma_{15'}$	3	$xy(x^2-y^2),\ yz(y^2-z^2),\ zx(z^2-x^2)$
$\Gamma_{25'}$	3	$xy,\ yz,\ zx$
$\Gamma_{1'}$	1	$xyz[x^4(y^2-z^2)+y^4(z^2-x^2)+z^4(x^2-y^2)]$
$\Gamma_{2'}$	1	xyz
$\Gamma_{12'}$	2	$xyz[z^2-\frac{1}{2}(x^2+y^2)],\ xyz(x^2-y^2)$
Γ_{15}	3	$x,\ y,\ z$
Γ_{25}	3	$z(x^2-y^2),\ x(y^2-z^2),\ y(z^2-x^2)$

1.4(14) Energy eigen values for $\boldsymbol{k} \cdot \boldsymbol{p}$ theory

Table: Energy eigenvalues used for energy band calculations by the $\boldsymbol{k} \cdot \boldsymbol{p}$ perturbation method in units of Rydbergs (from reference M. Cardona and F. H. Pollak: Phys. Rev. **142**, (1966) 530)

		germanium			silicon		
at $\boldsymbol{k} = 0$	waves	$\boldsymbol{k} \cdot \boldsymbol{p}$	OPW	pseudo	$\boldsymbol{k} \cdot \boldsymbol{p}$	OPW	pseudo
$\Gamma^l_{25'}$	[111]	0.00	0.00	0.00	0.00	0.00	0.00
$\Gamma^l_{2'}$	[111]	0.0728	−0.081	−0.007	0.265	0.164	0.23
Γ_{15}	[111]	0.232	0.231	0.272	0.252	0.238	0.28
Γ^u_1	[111]	0.571	0.571	0.444	0.520	0.692	0.52
Γ^l_1	[000]	−0.966	−0.929	−0.950	−0.950	−0.863	−0.97
$\Gamma_{12'}$	[200]	0.770	0.770	0.620	0.710	0.696	0.71
$\Gamma^u_{25'}$	[200]	1.25		0.890	0.940		0.94
$\Gamma^u_{2'}$	[200]	1.35		0.897	0.990		0.99

1.4(15) Momentum matrix elements used for $\boldsymbol{k}\cdot\boldsymbol{p}$ theory

Table: Momentum matrix elements used for the energy band calculations of germanium and silicon by the $\boldsymbol{k}\cdot\boldsymbol{p}$ perturbation (atomic units)

momentum matrix elements	germanium			silicon		
	$\boldsymbol{k}\cdot\boldsymbol{p}$	pseudo	c.r.	$\boldsymbol{k}\cdot\boldsymbol{p}$	pseudo	c.r.
$P = 2\mathrm{i}\langle\Gamma^l_{25'}\lvert\boldsymbol{p}\rvert\Gamma^l_{2'}\rangle$	1.360	1.24	1.36	1.200	1.27	1.20
$Q = 2\mathrm{i}\langle\Gamma^l_{25'}\lvert\boldsymbol{p}\rvert\Gamma_{15}\rangle$	1.070	0.99	1.07	1.050	1.05	1.05
$R = 2\mathrm{i}\langle\Gamma^l_{25'}\lvert\boldsymbol{p}\rvert\Gamma_{12'}\rangle$	0.8049	0.75	0.92	0.830	0.74	0.68
$P'' = 2\mathrm{i}\langle\Gamma^l_{25'}\lvert\boldsymbol{p}\rvert\Gamma^u_{2'}\rangle$	0.1000	0.09		0.100	0.10	
$P' = 2\mathrm{i}\langle\Gamma^u_{25'}\lvert\boldsymbol{p}\rvert\Gamma^l_{2'}\rangle$	0.1715	0.0092		−0.090	−0.10	
$Q' = 2\mathrm{i}\langle\Gamma^u_{25'}\lvert\boldsymbol{p}\rvert\Gamma_{15}\rangle$	−0.752	−0.65		−0.807	−0.64	
$R' = 2\mathrm{i}\langle\Gamma^u_{25'}\lvert\boldsymbol{p}\rvert\Gamma_{12'}\rangle$	1.4357	1.13		1.210	1.21	
$P''' = 2\mathrm{i}\langle\Gamma^u_{25'}\lvert\boldsymbol{p}\rvert\Gamma^u_{2'}\rangle$	1.6231	1.30		1.32	1.37	
$T = 2\mathrm{i}\langle\Gamma^u_{1}\lvert\boldsymbol{p}\rvert\Gamma_{15}\rangle$	1.2003	1.11		1.080	1.18	
$T' = 2\mathrm{i}\langle\Gamma^l_{1}\lvert\boldsymbol{p}\rvert\Gamma_{15}\rangle$	0.5323	0.41		0.206	0.34	

1.4(16) Decomposition of 15×15 $\boldsymbol{k} \cdot \boldsymbol{p}$ matrix (1)

(a) Δ_5 bands

Δ_5 bands: $(\Gamma_{15'}), \Gamma^u_{25'}, \Gamma^l_{25'}, \Gamma_{15}$

The matrix elements for these 3 bands are

$$\begin{array}{c} \begin{array}{ccc} |\Gamma^l_{25}\rangle & |\Gamma_{15}\rangle & |\Gamma^u_{25'}\rangle \end{array} \\ \left| \begin{array}{ccc} k_x^2 & Qk_x & 0 \\ Qk_x & \mathcal{E}(\Gamma_{15}) + k_x^2 & Q'k_x \\ 0 & Q'k_x & \mathcal{E}(\Gamma^u_{25'}) + k_x^2 \end{array} \right| \end{array} \tag{26}$$

(b) Δ_1 bands

Δ_1 bands: $\Gamma^l_1, \Gamma^u_1, (\Gamma_{12}), \Gamma_{15}$

The matrix elements for these three bands are

$$\begin{array}{c} \begin{array}{ccc} |\Gamma_{15}\rangle & |\Gamma^u_1\rangle & |\Gamma^l_1\rangle \end{array} \\ \left| \begin{array}{ccc} \mathcal{E}(\Gamma_{15}) + k_x^2 & Tk_x & T'k_x \\ Tk_x & \mathcal{E}(\Gamma^u_1) + k_x^2 & 0 \\ T'k_x & 0 & \mathcal{E}(\Gamma^l_1) + k_x^2 \end{array} \right| \end{array} \tag{27}$$

1.4(17) Decomposition of 15×15 $\boldsymbol{k} \cdot \boldsymbol{p}$ matrix (2)

(c) $\Delta_{2'}$ bands

$\Delta_{2'}$ bands: $\Gamma^l_{25'}, \Gamma^u_{25'}, \Gamma^l_{2'}, \Gamma^u_{2'}, \Gamma_{12'}$

The matrix elements for these five bands are

$$
\begin{array}{c}
\begin{array}{ccccc}
|\Gamma^l_{2'}\rangle & |\Gamma^l_{25'}\rangle & |\Gamma_{12'}\rangle & |\Gamma^u_{25'}\rangle & |\Gamma^u_{2'}
\end{array} \\
\left|\begin{array}{ccccc}
\mathcal{E}(\Gamma^l_{2'}) + k_x^2 & Pk_x & 0 & P'k_x & 0 \\
Pk_x & k_x^2 & \sqrt{2}Rk_x & 0 & P''k_x \\
0 & \sqrt{2}Rk_x & \mathcal{E}(\Gamma_{12'}) + k_x^2 & \sqrt{2}R'k_x & 0 \\
P'k_x & 0 & \sqrt{2}R'k_x & \mathcal{E}(\Gamma^u_{25'}) + k_x^2 & P'''k_x \\
0 & P''k_x & 0 & P'''k_x & \mathcal{E}(\Gamma^u_{2'}) + k_x^2
\end{array}\right|
\end{array}
\tag{28}
$$

1.4(18) Calculated results for Si and Ge

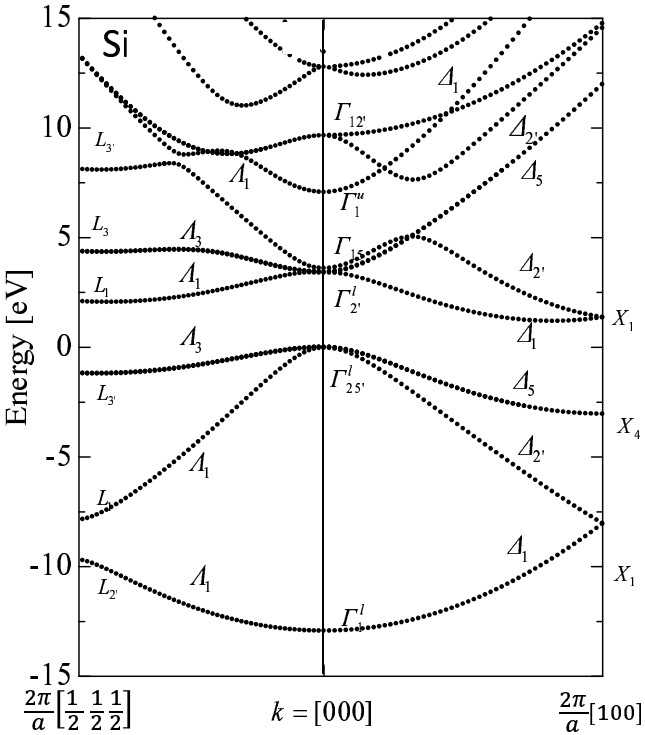

Figure: Energy band structure of Si calculated by 15×15 $\boldsymbol{k} \cdot \boldsymbol{p}$ method

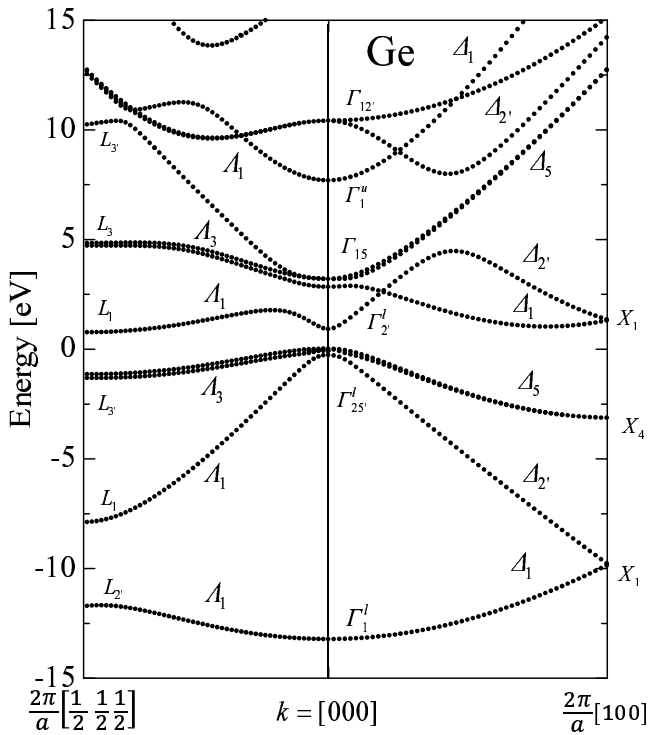

Figure: Energy band structure of Ge calculated by 15×15 $\boldsymbol{k} \cdot \boldsymbol{p}$ method with spin–orbit interaction

Spin–orbit interaction will be discussed in the next part.

Second part

1. Introduction to $\boldsymbol{k} \cdot \boldsymbol{p}$ perturbation and energy band calculations
   - 1.1 Bloch function
   - 1.2 $\boldsymbol{k} \cdot \boldsymbol{p}$ Hamiltonian
   - 1.3 Empty lattice bands and pseudopotential method
   - 1.4 $\boldsymbol{k} \cdot \boldsymbol{p}$ parameters and energy bands

2. Valence band analysis by $\boldsymbol{k} \cdot \boldsymbol{p}$ perturbation
   - 2.1 Second order $\boldsymbol{k} \cdot \boldsymbol{p}$ perturbation
   - 2.2 Spin-orbit interaction
   - 2.3 Dresselhaus Hamiltonian
   - 2.4 Valence bands dispersion and eigen states
   - 2.5 Luttinger Hamiltonian

2.1(1) Valence band analysis by $\boldsymbol{k}\cdot\boldsymbol{p}$ perturbation

We take account of the valence bands $\Gamma_{25'}$ and the conduction band $\Gamma_{2'}$ and then the matrix of the $\boldsymbol{k}\cdot\boldsymbol{p}$ Hamiltonian is given by

$$\begin{array}{c} |\Gamma_{2'}\rangle \\ \\ \mathcal{E}_c+\hbar^2k^2/2m \\ Pk_x \\ Pk_y \\ Pk_z \end{array} \begin{array}{c} |X\rangle \\ \\ Pk_x \\ \mathcal{E}_v+\hbar^2k^2/2m \\ 0 \\ 0 \end{array} \begin{array}{c} |Y\rangle \\ \\ Pk_y \\ 0 \\ \mathcal{E}_v+\hbar^2k^2/2m \\ 0 \end{array} \begin{array}{c} |Z\rangle \\ \\ Pk_z \\ 0 \\ 0 \\ \mathcal{E}_v+\hbar^2k^2/2m \end{array} \tag{29}$$

Next, from the above equation we obtain

$$\mathcal{E}_{1,2}=\frac{\mathcal{E}_c+\mathcal{E}_v}{2}\pm\sqrt{\left(\frac{\mathcal{E}_c-\mathcal{E}_v}{2}\right)^2+P^2k^2}+\frac{\hbar^2k^2}{2m} \tag{30}$$

$$\mathcal{E}_{3,4}=\mathcal{E}_v+\frac{\hbar^2k^2}{2m} \tag{31}$$

The bands $\mathcal{E}_{3,4}$ exhibit maxima at $\boldsymbol{k}=0$ and conflict with the actual valence bands.

2.1(2) Second–order perturbation

In the first part of this presentation, we discussed the mixing of 15 Γ states, which means that the valence bands $\Gamma_{25'}$ are mixed with many upper conduction bands $\Gamma_{2'}$, Γ_{15}, $\Gamma_{2'}$, and Γ_{12}. The second order perturbation terms play a very important role in the valence band analysis near $\boldsymbol{k} \simeq 0$. Then the energy is given by

$$\mathcal{E} = \frac{\hbar^2 k^2}{2m} + \sum_{i,j'} \frac{\langle j|H_1|i\rangle\langle i|H_1|j'\rangle}{\mathcal{E}_0 - \mathcal{E}_i} + \mathcal{E}_0 \tag{32}$$

where the eigenstates $|j\rangle$, $|j'\rangle$ are the triply-degenerate valence bands $\Gamma_{25'}$ ($|X\rangle$, $|Y\rangle$, $|Z\rangle$) with eigenvalue $\mathcal{E}_0$ and the eigenstates $|i\rangle$ correspond to any bands with eigenvalue $\mathcal{E}_i$ other than the valence bands $\Gamma_{25'}$.

2.1(3) Selection–rule

The upper four conduction bands appear in the matrix elements because of the the selection rules $\langle \Gamma_{25'} | \boldsymbol{p} | \Gamma_{l,j} \rangle$, where $\boldsymbol{p}$ is momentum vector and transforms as the representation Γ_{15} and $\Gamma_{l,j}$ are upper conduction band states. The direct product is given by using the character table of Table, (see the next page)

$$\Gamma_{25'} \times \Gamma_{15} = \Gamma_{12'} + \Gamma_{15} + \Gamma_{2'} + \Gamma_{25}$$

and thus only the conduction band states of the four representations on the right hand perturb the valence band edge.

2.1(4) Character table for fcc (O_h)

Table: Character table of small representations of O_h group

BSW	E	$3C_4^2$	$6C_4$	$6C_2$	$8C_3$	J	$3JC_4^2$	$6JC_4$	$6JC_2$	$8JC_3$
Γ_1	1	1	1	1	1	1	1	1	1	1
Γ_2	1	1	−1	−1	1	1	1	−1	−1	1
Γ_{12}	2	2	0	0	−1	2	2	0	0	−1
$\Gamma_{15'}$	3	−1	1	−1	0	3	−1	1	−1	0
$\Gamma_{25'}$	3	−1	−1	1	0	3	−1	−1	1	0
$\Gamma_{1'}$	1	1	1	1	1	−1	−1	−1	−1	−1
$\Gamma_{2'}$	1	1	−1	−1	1	−1	−1	1	1	−1
$\Gamma_{12'}$	2	2	0	0	-1	−2	−2	0	0	1
Γ_{15}	3	−1	1	−1	0	−3	1	−1	1	0
Γ_{25}	3	−1	−1	1	0	−3	1	1	−1	0
$\Gamma_{25'} \times \Gamma_{15}$	9	1	−1	−1	0	−9	−1	1	1	0
$\Gamma_{12'} + \Gamma_{15} + \Gamma_{2'} + \Gamma_{25}$	9	1	−1	−1	0	−9	−1	1	1	0

2.1(5) $\boldsymbol{k}\cdot\boldsymbol{p}$ method of Dresselhaus *et al.*

$$
\begin{aligned}
H_1 &= \frac{\hbar}{m}\boldsymbol{k}\cdot\boldsymbol{p} = -\mathrm{i}\frac{\hbar^2}{m}\left(k_x\frac{\partial}{\partial x}+k_y\frac{\partial}{\partial y}+k_x\frac{\partial}{\partial z}\right) \\
&= \frac{\hbar}{m}(k_x p_x + k_y p_y + k_z p_z) = \sum_{l=x,y,z}\frac{\hbar}{m}k_l p_l \qquad (33)
\end{aligned}
$$

Equation (32) is written as

$$
\begin{aligned}
\mathcal{E}(\boldsymbol{k}) &= \mathcal{E}_0 + \frac{\hbar^2k^2}{2m} + \frac{\hbar^2}{m^2}\sum_{l,m}\sum_{i,j'}\frac{\pi^l_{ji}\pi^m_{ij'}}{\mathcal{E}_0-\mathcal{E}_i}k_l k_m \\
&\equiv \mathcal{E}_0 + \sum_{l,m}\sum_{j'} D^{lm}_{jj'}k_l k_m \qquad (34)
\end{aligned}
$$

$$
\langle i|p_l|j\rangle = \pi^l_{ij} \qquad (35)
$$

$$
D^{lm}_{jj'} = \frac{\hbar^2}{2m}\delta_{jj'}\delta_{lm} + \frac{\hbar^2}{m^2}\sum_i\frac{\pi^l_{ji}\pi^m_{ij'}}{\mathcal{E}_0-\mathcal{E}_i} \qquad (36)
$$

2.1(6) $\boldsymbol{k}\cdot\boldsymbol{p}$ matrix define by Dresselhaus *et al.*

From these results, the matrix elements of the $\boldsymbol{k}\cdot\boldsymbol{p}$ Hamiltonian are given by

$$\begin{array}{c|ccc} & |X\rangle & |Y\rangle & |Z\rangle \\ \langle X| & Ak_x^2 + B(k_y^2+k_z^2) & Ck_xk_y & Ck_xk_z \\ \langle Y| & Ck_xk_y & Ak_y^2 + B(k_x^2+k_z^2) & Ck_yk_z \\ \langle Z| & Ck_xk_z & Ck_yk_z & Ak_z^2 + B(k_x^2+k_y^2) \end{array} \tag{37}$$

The three terms of A, B, and C are defined by Luttinger which are related to L, M, and$N$ defined by Dresselhaus, Kip and Kittel.

$$A = \frac{\hbar^2}{2m} + \frac{\hbar^2}{m^2}\sum_i \frac{\pi_{Xi}^x \pi_{iX}^x}{\mathcal{E}_0 - \mathcal{E}_i} = \frac{\hbar^2}{2m} + L \tag{38a}$$

$$B = \frac{\hbar^2}{2m} + \frac{\hbar^2}{m^2}\sum_i \frac{\pi_{Xi}^y \pi_{iX}^y}{\mathcal{E}_0 - \mathcal{E}_i} = \frac{\hbar^2}{2m} + M \tag{38b}$$

$$C = \frac{\hbar^2}{m^2}\sum_i \frac{\pi_{Xi}^x \pi_{iY}^y + \pi_{Xi}^y \pi_{iY}^x}{\mathcal{E}_0 - \mathcal{E}_i} = N \tag{38c}$$

2.1(7) Valence band structure

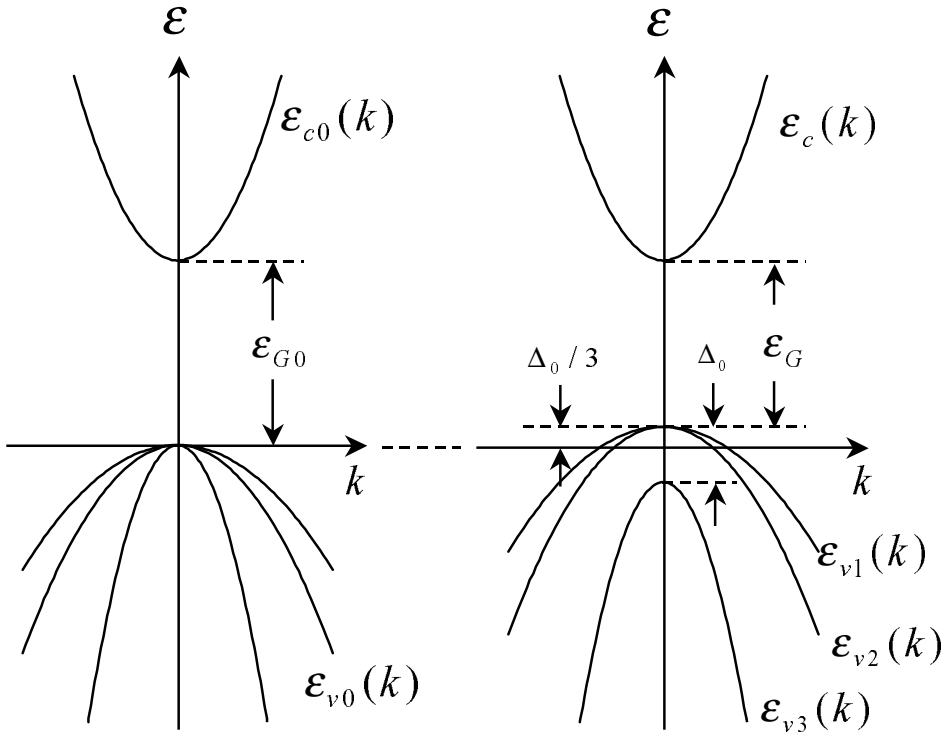

Figure: Valence band structure. The left figure shows the splitting of the valence bands at $\boldsymbol{k} \neq 0$ due to the interaction between the bands, and the right figure shows the valence band structures obtained by taking the spin–orbit interaction into account, where the heavy hole and light hole bands are doubly-degenerate at $\boldsymbol{k} = 0$ and the lowest band is the spin–orbit split-off band due to the spin–orbit interaction.

2.2(1) Spin–orbit interaction

Electron has spin magnetic moment $\boldsymbol{\mu}_{\mathrm{S}}$ and interact with the angular momentum $\boldsymbol{L}$. Semiclassical interpretation of the spin–orbit interaction is made by the figure shown below;

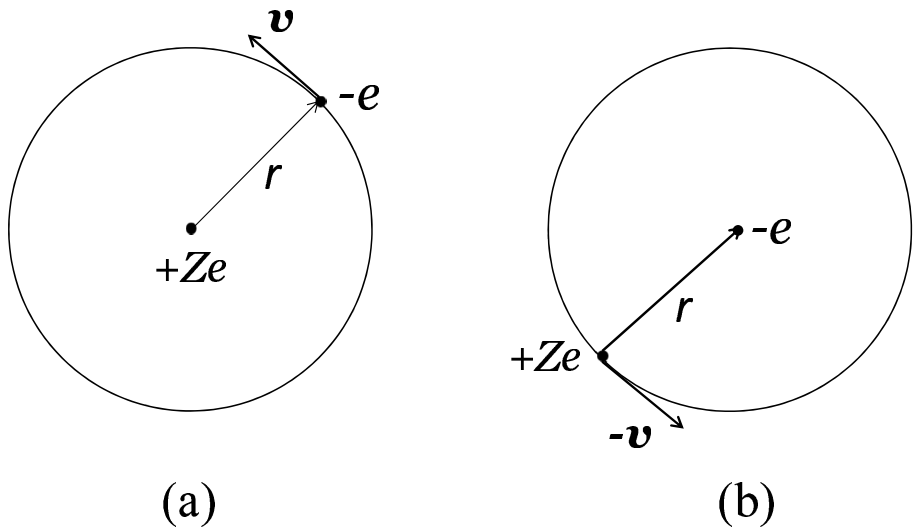

Figure: (a) Bohr orbital motion of an electron $-e$ with the velocity $\boldsymbol{v}$ as seen by the nucleus Ze is interpreted from the point of view of the electron as (b) the nucleus Ze is moving with velocity $-\boldsymbol{v}$ around the electron

2.2(2) Semiclassical derivation of spin-orbit interaction

The nucleus of charge Ze moving with velocity $-\boldsymbol{v}$ will produce a current

$$\boldsymbol{j} = -Ze\boldsymbol{v} \quad \text{[SI]} \tag{39}$$

The charge motion produces a magnetic field at the position of the electron, which is given by Biot-Sabart law,

$$\boldsymbol{B} = \frac{\mu_0}{4\pi}\frac{\boldsymbol{j}\times\boldsymbol{r}}{r^3} = -\frac{\mu_0 Ze}{4\pi}\frac{\boldsymbol{v}\times\boldsymbol{r}}{r^3} \quad \text{[SI]} \tag{40}$$

Electric field $\boldsymbol{E}$ acting on the electron is given by Coulomb's law

$$\boldsymbol{E} = +\frac{Ze}{4\pi\epsilon_0}\frac{\boldsymbol{r}}{r^3} \quad \text{[SI]} \tag{41}$$

Therefore the magnetic field is given by

$$\boldsymbol{B} = -\frac{1}{c^2}\boldsymbol{v}\times\boldsymbol{E} \quad \text{[SI]} \tag{42}$$

2.2(3) Semiclassical derivation of spin-orbit interaction

The magnetic field given by (40) interacts with the spin magnetic moment $\boldsymbol{\mu}_{\mathrm{S}}$,

$$\boldsymbol{\mu}_{\mathrm{S}} \;=\; -2\frac{\mu_{\mathrm{B}}}{\hbar}\boldsymbol{S} = -\frac{e}{m}\boldsymbol{S} \quad [\mathrm{SI}] \tag{43}$$

where the approximated factor 2 is used instead of the observed value $\simeq 2.002319$ and $\mu_{\mathrm{B}} = e\hbar/2m$ is called Bohr magneton.
The interaction energy is evaluated as the scalar product of the magnetic moment and the magnetic field acting on the electron, and thus using (42)

$$\begin{aligned} H_{\mathrm{so}} &= -\frac{1}{2}\boldsymbol{\mu}_{\mathrm{S}} \cdot \left(\frac{1}{c^2}\boldsymbol{v}\times\boldsymbol{E}\right) = \frac{1}{2}\frac{\boldsymbol{\mu}_{\mathrm{S}}}{m}\cdot(\boldsymbol{E}\times\boldsymbol{p}) \\ &= -\frac{1}{2}\frac{1}{mc^2}\frac{1}{r}\frac{\mathrm{d}\phi}{\mathrm{d}r}(\boldsymbol{r}\times\boldsymbol{p})\cdot\boldsymbol{\mu}_{\mathrm{S}} = -\frac{e}{2m^2c^2}\frac{1}{r}\frac{\mathrm{d}\phi}{\mathrm{d}r}\boldsymbol{L}\cdot\boldsymbol{S} \\ &= \frac{1}{2m^2c^2}\frac{1}{r}\frac{\mathrm{d}V}{\mathrm{d}r}\boldsymbol{L}\cdot\boldsymbol{S} \end{aligned} \tag{44}$$

2.2(4) Spin-orbit interaction Hamiltonian

Using Pauli spin operator $\boldsymbol{\sigma}$ ($\boldsymbol{S} = (\hbar/2)\boldsymbol{\sigma}$), the above spin–orbit Hamiltonian is rewritten as

$$H_{\mathrm{so}} \propto \boldsymbol{L} \cdot \boldsymbol{\sigma} = (\boldsymbol{r} \times \boldsymbol{p}) \cdot \boldsymbol{\sigma} = -\mathrm{i}\hbar(\boldsymbol{r} \times \nabla) \cdot \boldsymbol{\sigma} \tag{45}$$

and we find that

$$-\mathrm{i}\hbar(\boldsymbol{r} \times \nabla) \cdot \boldsymbol{\sigma} = -\mathrm{i}\left[\left(y\frac{\partial}{\mathrm{d}z} - z\frac{\partial}{\mathrm{d}y}\right)\sigma_x + \left(z\frac{\partial}{\mathrm{d}x} - x\frac{\partial}{\mathrm{d}z}\right)\sigma_y + \left(x\frac{\partial}{\mathrm{d}y} - y\frac{\partial}{\mathrm{d}x}\right)\sigma_z\right]$$

$$\begin{aligned} \langle\uparrow|\sigma_x|\downarrow\rangle &= \langle\downarrow|\sigma_x|\uparrow\rangle = 1 \\ \langle\uparrow|\sigma_y|\downarrow\rangle &= -\mathrm{i},\ \langle\downarrow|\sigma_y|\uparrow\rangle = \mathrm{i} \\ \langle\uparrow|\sigma_z|\uparrow\rangle &= 1,\ \langle\downarrow|\sigma_z|\downarrow\rangle = -1 \end{aligned} \tag{46}$$

2.2(5) Matrix elements of H_{so} for $\Gamma_{25'}$ valence bands

Choosing the wave functions $|X\uparrow\rangle$, $|Y\uparrow\rangle$, and $|Z\downarrow\rangle$ for $\Gamma^l_{25'}$, the spin–orbit interaction is given by

$$\langle\uparrow X(\Gamma_{25'})|H_{\rm so}|Y(\Gamma_{25'})\uparrow\rangle = -{\rm i}\Delta_{25'}/3 \quad (47)$$

$$\langle\uparrow X(\Gamma_{25'})|H_{\rm so}|Z(\Gamma_{25'})\downarrow\rangle = +\Delta_{25'}/3 \quad (48)$$

$$\langle\uparrow Y(\Gamma_{25'})|H_{\rm so}|Z(\Gamma_{25'})\downarrow\rangle = -{\rm i}\Delta_{25'}/3 \quad (49)$$

$$\begin{array}{c} \begin{array}{ccc} |X\uparrow\rangle & |Y\uparrow\rangle & |Z\downarrow\rangle \end{array} \\ \left|\begin{array}{ccc} 0 & -{\rm i}\Delta_{25'}/3 & \Delta_{25'}/3 \\ {\rm i}\Delta_{25'}/3 & 0 & -{\rm i}\Delta_{25'}/3 \\ \Delta_{25'}/3 & {\rm i}\Delta_{25'}/3 & 0 \end{array}\right| \end{array} \left|\begin{array}{c} |X\uparrow\rangle \\ |Y\uparrow\rangle \\ |Z\downarrow\rangle \end{array}\right| \quad (50)$$

2.2(6) Spin–orbit splitting

and diagonalization results in

$$\begin{vmatrix} -(2/3)\Delta_{25'} & 0 & 0 \\ 0 & (1/3)\Delta_{25'} & 0 \\ 0 & 0 & (1/3)\Delta_{25'} \end{vmatrix} \begin{vmatrix} u_{v3} \\ u_{v2} \\ u_{v1} \end{vmatrix} \tag{51}$$

Therefore the spin–orbit splitting of $\Gamma_{25'}$ bands is $\Delta_0 = \Delta_{25'}$ and the corresponding eigenfunctions are

$$\begin{aligned} u_{v3} &= \frac{1}{\sqrt{3}}\left(-|X\uparrow\rangle + \mathrm{i}|Y\uparrow\rangle + |Z\downarrow\rangle\right) \\ u_{v2} &= \frac{1}{\sqrt{2}}\left(|X\uparrow\rangle + |Z\downarrow\rangle\right) \\ u_{v1} &= \frac{1}{\sqrt{2}}\left(-\mathrm{i}|X\uparrow\rangle + |Y\uparrow\rangle\right) \end{aligned}$$

2.3(1) 6×6 $\boldsymbol{k} \cdot \boldsymbol{p}$ Dresselhaus Hamiltonian

Here the spin states $S_z = +\hbar/2$ and $S_z = -\hbar/2$ are sometimes referred to as $\uparrow$ spin and $\downarrow$ spin and their eigenstates are

$$|\uparrow\rangle = |\alpha\rangle = \begin{bmatrix} 1 \\ 0 \end{bmatrix}, \quad |\downarrow\rangle = |\beta\rangle = \begin{bmatrix} 0 \\ 1 \end{bmatrix}. \tag{52}$$

Next, we define the angular momentum operators for the $\Gamma_{25'}$ valence bands. As stated before the eigenstates of the valence bands at $\boldsymbol{k} = 0$ are expressed by $|X\rangle$, $|Y\rangle$, $|Z\rangle$. Their angular momentum $\boldsymbol{L} = \boldsymbol{r} \times \boldsymbol{p}$ has a quantum number of unity and the matrix representation of the operator is

$$L_x = \frac{\hbar}{\sqrt{2}} \begin{bmatrix} 0 & 1 & 0 \\ 1 & 0 & 1 \\ 0 & 1 & 0 \end{bmatrix}, L_y = \frac{\hbar}{\sqrt{2}} \begin{bmatrix} 0 & -\mathrm{i} & 0 \\ \mathrm{i} & 0 & -\mathrm{i} \\ 0 & \mathrm{i} & 0 \end{bmatrix}, L_z = \hbar \begin{bmatrix} 1 & 0 & 0 \\ 0 & 0 & 0 \\ 0 & 0 & -1 \end{bmatrix} \tag{53}$$

$$|\uparrow\rangle = |\alpha\rangle = \begin{bmatrix} 1 \\ 0 \end{bmatrix}, \quad |\downarrow\rangle = |\beta\rangle = \begin{bmatrix} 0 \\ 1 \end{bmatrix} \tag{54}$$

2.3(2) New representation of $\Gamma_{25'}$ valence bands

When we choose the basis of the eigenstates defined by

$$u_+ = \frac{1}{\sqrt{2}}(|X\rangle + \mathrm{i}|Y\rangle) = \begin{bmatrix} 1 \\ 0 \\ 0 \end{bmatrix}, \tag{55a}$$

$$u_- = \frac{1}{\sqrt{2}}(|X\rangle - \mathrm{i}|Y\rangle) = \begin{bmatrix} 0 \\ 0 \\ 1 \end{bmatrix}, \tag{55b}$$

$$u_z = |Z\rangle = \begin{bmatrix} 0 \\ 1 \\ 0 \end{bmatrix}, \tag{55c}$$

the angular momentum operators are given by

$$L_\pm = L_x \pm \mathrm{i}L_y\,, \tag{56}$$

where

$$L_+ = \sqrt{2}\hbar \begin{bmatrix} 0 & 1 & 0 \\ 0 & 0 & 1 \\ 0 & 0 & 0 \end{bmatrix}, \quad L_- = \sqrt{2}\hbar \begin{bmatrix} 0 & 0 & 0 \\ 1 & 0 & 0 \\ 0 & 1 & 0 \end{bmatrix}. \tag{57}$$

2.3(3) 6×6 matrix elements of spin–orbit interaction

Similarly, the spin momentum operators are expressed as

$$\sigma_{\pm} = \sigma_x \pm \mathrm{i}\sigma_y \,, \tag{58}$$

and their matrix representations are given by

$$\sigma_+ = 2\begin{bmatrix} 0 & 1 \\ 0 & 0 \end{bmatrix}, \quad \sigma_- = 2\begin{bmatrix} 0 & 0 \\ 1 & 0 \end{bmatrix}. \tag{59}$$

The six states of the valence bands $|u_+\alpha\rangle$, $|u_+\beta\rangle$, $|u_z\alpha\rangle$, $|u_-\beta\rangle$, $|u_-\alpha\rangle$, $|u_z\beta\rangle$ give rise to the matrix elements of the spin–orbit interaction Hamiltonian at $\boldsymbol{k} = 0$:

$$\begin{array}{c} u_+\alpha \quad u_+\beta \quad u_z\alpha \quad u_-\beta \quad u_-\alpha \quad u_z\beta \\ \left|\begin{array}{cccccc} \Delta & 0 & 0 & 0 & 0 & 0 \\ 0 & -\Delta & \sqrt{2}\Delta & 0 & 0 & 0 \\ 0 & \sqrt{2}\Delta & 0 & 0 & 0 & 0 \\ 0 & 0 & 0 & \Delta & 0 & 0 \\ 0 & 0 & 0 & 0 & -\Delta & \sqrt{2}\Delta \\ 0 & 0 & 0 & 0 & \sqrt{2}\Delta & 0 \end{array}\right| \end{array}. \tag{60}$$

2.3(4) Diagonalization of spin–orbit Hamiltonian matrix

Diagonalization of the matrix gives rise to the following result.

$$\begin{vmatrix} \Delta & 0 & 0 & 0 & 0 & 0 \\ 0 & \Delta & 0 & 0 & 0 & 0 \\ 0 & 0 & -2\Delta & 0 & 0 & 0 \\ 0 & 0 & 0 & \Delta & 0 & 0 \\ 0 & 0 & 0 & 0 & \Delta & 0 \\ 0 & 0 & 0 & 0 & 0 & -2\Delta \end{vmatrix} . \tag{61}$$

2.3(5) Eigen states of the valence bands with spin–orbit interaction

$$
\begin{aligned}
u_{v1} &= \left|\frac{3}{2},\frac{3}{2}\right\rangle = \sqrt{\frac{1}{2}}\,|(X+\mathrm{i}Y)\uparrow\rangle\ , \\
u_{v2} &= \left|\frac{3}{2},\frac{1}{2}\right\rangle = \mathrm{i}\sqrt{\frac{1}{6}}\,[|(X+\mathrm{i}Y)\downarrow\rangle - 2\,|Z\uparrow\rangle]\,, \\
u_{v3} &= \left|\frac{1}{2},\frac{1}{2}\right\rangle = \sqrt{\frac{1}{3}}\,[|(X+\mathrm{i}Y)\downarrow\rangle + |Z\uparrow\rangle]\,, \\
u_{v1'} &= \left|\frac{3}{2},-\frac{3}{2}\right\rangle = \mathrm{i}\sqrt{\frac{1}{2}}\,|(X-\mathrm{i}Y)\downarrow\rangle\ , \\
u_{v2'} &= \left|\frac{3}{2},-\frac{1}{2}\right\rangle = \sqrt{\frac{1}{6}}\,[|(X-\mathrm{i}Y)\uparrow\rangle + 2\,|Z\downarrow\rangle]\,, \\
u_{v3'} &= \left|\frac{1}{2},-\frac{1}{2}\right\rangle = \mathrm{i}\sqrt{\frac{1}{3}}\,[-|(X-\mathrm{i}Y)\uparrow\rangle + |Z\downarrow\rangle]\ .
\end{aligned}
$$

2.4(1) Valence bands: Definition of Dresselhaus *et al*

The matrix elements of the Hamiltonian with the spin–orbit interaction. Defining the matrix element H_{ij} by

$$\begin{aligned} H_{11} &= Lk_x^2 + M(k_y^2 + k_z^2)\,, \\ H_{22} &= Lk_y^2 + M(k_z^2 + k_x^2)\,, \\ H_{33} &= Lk_z^2 + M(k_x^2 + k_y^2)\,, \\ H_{12} &= Nk_xk_y\,, \\ H_{23} &= Nk_yk_z\,, \\ H_{13} &= Nk_xk_z\,. \end{aligned}$$

The result is given by the 6×6 matrix of (62) in the paper of Dresselhaus et al.

2.4(2) 6×6 matrix of $\Gamma_{25'}$ valence bands

$$
\begin{vmatrix}
\frac{H_{11}+H_{22}}{2} & -\frac{H_{13}-\mathrm{i}H_{23}}{\sqrt{3}} & -\frac{H_{11}-H_{22}-2\mathrm{i}H_{12}}{2\sqrt{3}} \\
-\frac{H_{13}+\mathrm{i}H_{23}}{\sqrt{3}} & \frac{4H_{33}+H_{11}+H_{22}}{6} & 0 \\
-\frac{H_{11}-H_{22}+2\mathrm{i}H_{12}}{2\sqrt{3}} & 0 & \frac{4H_{33}+H_{11}+H_{22}}{6} \\
0 & -\frac{H_{11}-H_{22}+2\mathrm{i}H_{12}}{2\sqrt{3}} & \frac{H_{13}+\mathrm{i}H_{23}}{\sqrt{3}} \\
-\frac{H_{13}+\mathrm{i}H_{23}}{\sqrt{6}} & -\frac{H_{11}+H_{22}-2H_{33}}{3\sqrt{2}} & \frac{H_{13}-\mathrm{i}H_{23}}{\sqrt{2}} \\
-\frac{H_{11}-H_{22}+2\mathrm{i}H_{12}}{\sqrt{6}} & \frac{H_{13}+\mathrm{i}H_{23}}{\sqrt{2}} & \frac{H_{11}+H_{22}-2H_{33}}{3\sqrt{2}}
\end{vmatrix}
$$

$$
\begin{vmatrix}
0 & -\frac{H_{13}-\mathrm{i}H_{23}}{\sqrt{6}} & -\frac{H_{11}-H_{22}-2\mathrm{i}H_{12}}{\sqrt{6}} \\
-\frac{H_{11}-H_{22}-2\mathrm{i}H_{12}}{2\sqrt{3}} & -\frac{H_{11}+H_{22}-2H_{33}}{3\sqrt{2}} & \frac{H_{13}-\mathrm{i}H_{23}}{\sqrt{2}} \\
\frac{H_{13}-\mathrm{i}H_{23}}{\sqrt{3}} & \frac{H_{13}+\mathrm{i}H_{23}}{\sqrt{2}} & \frac{H_{11}+H_{22}-2H_{33}}{3\sqrt{2}} \\
\frac{H_{11}+H_{22}}{2} & \frac{H_{11}-H_{22}+2\mathrm{i}H_{12}}{\sqrt{6}} & -\frac{H_{13}+\mathrm{i}H_{23}}{\sqrt{6}} \\
\frac{H_{11}-H_{22}-2\mathrm{i}H_{12}}{\sqrt{6}} & \frac{H_{11}+H_{22}+H_{33}}{3}-\Delta_0 & 0 \\
-\frac{H_{13}-\mathrm{i}H_{23}}{\sqrt{6}} & 0 & \frac{H_{11}+H_{22}+H_{33}}{3}-\Delta_0
\end{vmatrix}.
$$

2.4(3) Valence band dispersion at $\boldsymbol{k} \simeq 0$

The matrix is approximately divided into two matrices comprising the upper-left 4×4 matrix and the lower-right 2×2 matrix. The 4×4 matrix gives the solutions of

$$\mathcal{E}(\boldsymbol{k}) = Ak^2 \pm \sqrt{B^2k^4 + C^2(k_x^2k_y^2 + k_y^2k_z^2 + k_z^2k_x^2)}\,, \qquad (62)$$

$$\begin{aligned} A &= \frac{1}{3}(L + 2M), \\ B &= \frac{1}{3}(L - M), \\ C &= \frac{1}{3}[N^2 - (L - M)^2]\,. \end{aligned} \qquad (63)$$

On the other hand, from the 2×2 matrix we obtain the solutions

$$\mathcal{E}(\boldsymbol{k}) = Ak^2 - \Delta_0\,. \qquad (64)$$

2.4(4) Warped energy surfaces

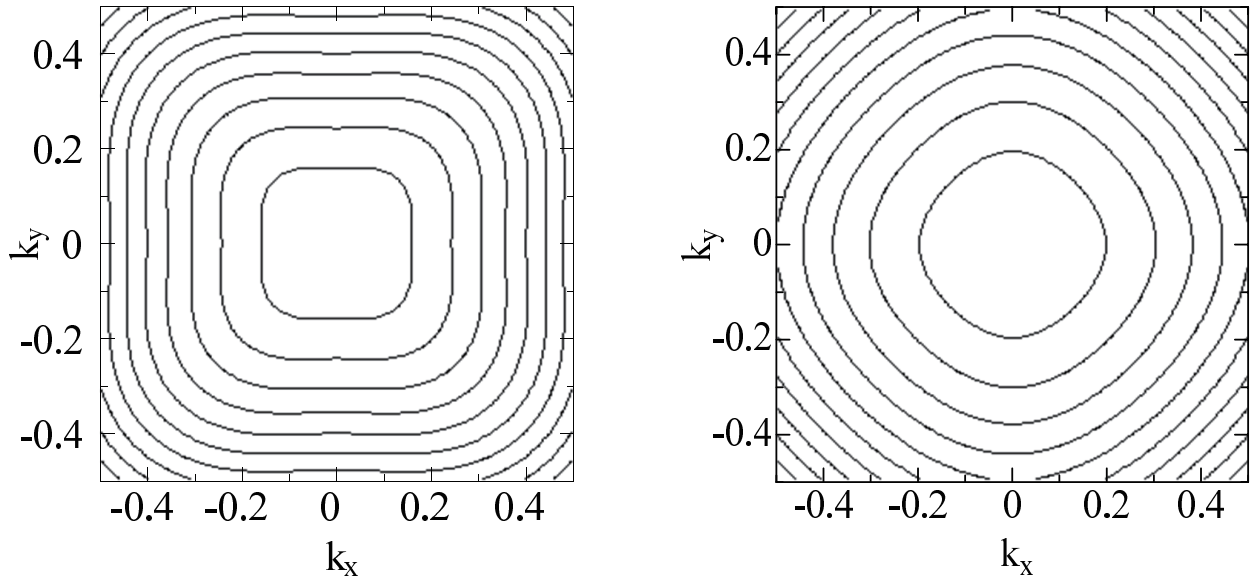

Figure: Energy contour lines of (a) the heavy–hole and (b) light–hole valence bands in the (001) plane of Si

2.5(1) Dresselhaus vs. Luttinger Hamiltonian

From (62) we obtain the following matrix elements

$$\frac{H_{11}+H_{22}}{2} = \frac{L+M}{2}(k_x^2+k_y^2) + Mk_z^2 \left(= \frac{1}{2}P(\boldsymbol{k})\right) ,$$

$$-\frac{H_{13}-\mathrm{i}H_{23}}{\sqrt{3}} = -\frac{N}{\sqrt{3}}(k_x-\mathrm{i}k_y)k_z \,(= L(\boldsymbol{k})) ,$$

$$-\frac{H_{11}-H_{22}-2\mathrm{i}H_{12}}{2\sqrt{3}} = \frac{(L-M)(k_x^2-k_y^2)-2\mathrm{i}Nk_xk_y}{\sqrt{12}} \,(= M(\boldsymbol{k})) ,$$

$$\frac{H_{33}+H_{11}+H_{22}}{6} = \frac{1}{6}\left[(L+M)(k_x^2+k_y^2)P + 2Mk_z^2\right] + \frac{2}{3}M(k_x^2+k_y^2) + Lk_z^2 \left(= \frac{1}{6}P(\boldsymbol{k}) + \frac{2}{3}Q(\boldsymbol{k})\right) ,$$

2.5(2) 6 bands $\boldsymbol{k}\cdot\boldsymbol{p}$ Hamiltonian

$\lvert\frac{3}{2},\frac{3}{2}\rangle$	$P/2$	L	M	0	$\mathrm{i}L/\sqrt{2}$	$-\mathrm{i}\sqrt{2}M$
$\lvert\frac{3}{2},\frac{1}{2}\rangle$	L^*	$P/6+2Q/3$	0	M	$-\mathrm{i}(P-2Q)/3\sqrt{2}$	$\mathrm{i}\sqrt{3/}L$
$\lvert\frac{3}{2},-\frac{1}{2}\rangle$	M^*	0	$P/6+2Q/3$	$-L$	$-\mathrm{i}\sqrt{3/2}L^*$	$-\mathrm{i}(P-2Q)/3\sqrt{2}$
$\lvert\frac{3}{2},-\frac{3}{2}\rangle$	0	M^*	$-L^*$	$P/2$	$-\mathrm{i}\sqrt{2}M^*$	$-\mathrm{i}L^*/\sqrt{2}$
$\lvert\frac{1}{2},\frac{1}{2}\rangle$	$-\mathrm{i}L^*/\sqrt{2}$	$\mathrm{i}(P-2Q)/3\sqrt{2}$	$\mathrm{i}\sqrt{3/2}L$	$\mathrm{i}\sqrt{2}M$	$(P+Q)/3-\Delta_0$	0
$\lvert\frac{1}{2},-\frac{1}{2}\rangle$	$\mathrm{i}\sqrt{2}M^*$	$-\mathrm{i}\sqrt{3/2}L^*$	$\mathrm{i}(P-2Q)/3\sqrt{2}$	$\mathrm{i}L/\sqrt{2}$	0	$(P+Q)/3-\Delta_0$

$$
\begin{aligned}
P(\boldsymbol{k}) &= \frac{\hbar^2}{2m}\left[(A+B)(k_x^2+k_y^2)+2Bk_z^2\right] , \\
L(\boldsymbol{k}) &= -\mathrm{i}\frac{C}{\sqrt{3}}\frac{\hbar^2}{2m}(k_x-\mathrm{i}k_y))k_s , \\
Q(\boldsymbol{k}) &= \frac{\hbar^2}{2m}\left[B(k_x^2+k_y^2)+A\frac{\hbar^2}{2m}k_z^2\right] , \\
M(\boldsymbol{k}) &= \frac{1}{\sqrt{12}}\frac{\hbar^2}{2m}\left[(A-B)(k_x^2-k_y^2)-2\mathrm{i}k_xk_y\right] ,
\end{aligned}
$$

2.5(3) Luttinger parameters

Relation between Luttinger parameters γ_1, γ_2, γ_3 and A, B, C:

$$\begin{aligned} \gamma_1 &= -\frac{1}{3}(A+2B)\,, \quad \gamma_2 = -\frac{1}{6}(A-B)\,, \quad \gamma_3 = -\frac{1}{6}C\,, \\ -A &= \gamma_1 + 4\gamma_2\,, \quad -B = \gamma_1 - 2\gamma_2\,, \quad -C = 6\gamma_3\,. \end{aligned}$$

When the matrix elements are redefined as

$$\begin{aligned} P' &= \frac{1}{3}(P+Q) = -\gamma_1 \frac{\hbar^2}{2m}(k_x^2 + k_y^2 + k_z^2)\,, \\ Q' &= \frac{1}{6}(P-2Q) = -\gamma_2 \frac{\hbar^2}{2m}(k_x^2 + k_y^2 - 2k_z^2)\,, \\ L &= \mathrm{i}2\sqrt{3}\gamma_3 \frac{\hbar^2}{2m}(k_x - \mathrm{i}k_y)k_z\,, \\ M &= -\sqrt{3}\frac{\hbar^2}{2m}\left[\gamma_2(k_x^2 - k_y^2) - 2\mathrm{i}\gamma_3 k_x k_y\right]\,, \end{aligned}$$

2.5(4) 6×6 Luttinger Hamiltonian

6×6 Luttinger Hamiltonian is written as:

$$\begin{vmatrix} P'+Q' & L & M & 0 & \mathrm{i}L/\sqrt{2} & -\mathrm{i}\sqrt{2}M \\ L^* & P'-Q' & 0 & M & -\mathrm{i}\sqrt{2}Q' & \mathrm{i}\sqrt{3/2}L \\ M^* & 0 & P'-Q' & -L & -\mathrm{i}\sqrt{3/2}L^* & -\mathrm{i}\sqrt{2}Q' \\ 0 & M^* & -L^* & P'+Q' & -\mathrm{i}\sqrt{2}M^* & -\mathrm{i}L^*/\sqrt{2} \\ -\mathrm{i}L^*/\sqrt{2} & \mathrm{i}\sqrt{2}Q' & \mathrm{i}\sqrt{3/2}L & \mathrm{i}\sqrt{2}M & P'-\Delta_0 & 0 \\ \mathrm{i}\sqrt{2}M^* & -\mathrm{i}\sqrt{3/2}L^* & \mathrm{i}\sqrt{2}Q' & \mathrm{i}L/\sqrt{2} & 0 & P'-\Delta_0 \end{vmatrix}.$$

2.5(6) 8×8 $\boldsymbol{k} \cdot \boldsymbol{p}$ Hamiltonian

$$
\begin{vmatrix}
T & 0 & U & -\mathrm{i}\sqrt{2}V & U^*/\sqrt{3} & 0 & V & -\mathrm{i}\sqrt{2/3}U^* \\
0 & T & 0 & \mathrm{i}U/\sqrt{3} & \sqrt{2}V & \mathrm{i}U^* & \sqrt{2/3}U & \mathrm{i}V \\
U^* & 0 & P'+Q' & L & M & 0 & \mathrm{i}L/\sqrt{2} & -\mathrm{i}\sqrt{2}M \\
\mathrm{i}\sqrt{2}V & -\mathrm{i}U^*/\sqrt{3} & L^* & P'-Q' & 0 & M & -\mathrm{i}\sqrt{2}Q' & \mathrm{i}\sqrt{3/2}L \\
U/\sqrt{3} & \sqrt{2}V & M^* & 0 & P'-Q' & -L & -\mathrm{i}\sqrt{3}L^*/\sqrt{2} & -\mathrm{i}\sqrt{2}Q' \\
0 & -\mathrm{i}U & 0 & M^* & -L^* & P'+Q' & -\mathrm{i}\sqrt{2}M^* & -\mathrm{i}L^*/\sqrt{2} \\
V & \sqrt{2/3}U^* & -\mathrm{i}L^*/\sqrt{2} & \mathrm{i}\sqrt{2}Q' & \mathrm{i}\sqrt{3/2}L & \mathrm{i}\sqrt{2}M & P'-\Delta_0 & 0 \\
\mathrm{i}\sqrt{2/3}U & -\mathrm{i}V & -\mathrm{i}\sqrt{2}M^* & -\mathrm{i}\sqrt{3/2}L^* & \mathrm{i}\sqrt{2}Q' & \mathrm{i}L/\sqrt{2} & 0 & P'-\Delta_0
\end{vmatrix}
$$

$$
\begin{aligned}
T &= \mathcal{E}_c + \frac{\hbar^2}{2m}(k_x^2 + k_y^2 + k_z^2)\,, \\
U &= \frac{1}{\sqrt{2}}\frac{\hbar}{m}P_0(k_x + \mathrm{i}k_y)\,, \\
V &= \frac{1}{\sqrt{3}}\frac{\hbar}{m}P_0 k_z\,, \\
P_0 &= \langle \Gamma_{2'}|p_x|\Gamma_{25'}(X)\rangle\,,
\end{aligned}
$$

2.5(7) Kane's parameters

$$\Gamma_{25'} \times \Gamma_{15} = \Gamma_{12'} + \Gamma_{15} + \Gamma_{2'} + \Gamma_{25}$$

This relation shows four conduction band states perturb the valence band edge.

$$\begin{aligned}
F &= -\frac{2}{m}\sum_j \frac{|\langle \Gamma_{25'}(X)|p_x|\Gamma_{2'}, j\rangle|^2}{\mathcal{E}_j} \\
G &= -\frac{2}{m}\sum_j \frac{|\langle \Gamma_{25'}(X)|p_x|\Gamma_{12'}, j\rangle|^2}{\mathcal{E}_j} \\
H_1 &= -\frac{2}{m}\sum_j \frac{|\langle \Gamma_{25'}(X)|p_y|\Gamma_{15}, j\rangle|^2}{\mathcal{E}_j} \\
H_2 &= -\frac{2}{m}\sum_j \frac{|\langle \Gamma_{25'}(X)|p_y|\Gamma_{25}, j\rangle|^2}{\mathcal{E}_j} \\
\gamma_1 &= -\frac{1}{3}(F + 2G + 2H_1 + 2H_2) - 1 \\
\gamma_2 &= -\frac{1}{6}(F + 2G - H_1 - H_2) \\
\gamma_3 &= -\frac{1}{6}(F - G + H_1 - H_2)
\end{aligned}$$

2.5(8) Luttinger parameters

$$F = \frac{2}{m}\sum_j \frac{|\langle \Gamma_{25'}(X)|p_x|\Gamma_{2'}\rangle|^2}{\mathcal{E}_v - \mathcal{E}_j} = -\frac{\mathcal{E}_P}{3}\left[\frac{2}{\mathcal{E}_G} + \frac{1}{\mathcal{E}_G + \Delta_0}\right].$$

Since the 8×8 $\boldsymbol{k}\cdot\boldsymbol{p}$ Hamiltonian includes the coupling between the conduction band $|\Gamma_{2'}\rangle$ and the valence bands $|\Gamma_{25'}\rangle$, we have to exclude the contributions from the conduction band $|\Gamma_{2'}\rangle$, the term F. We redefine the Luttinger parameters as γ_1^L, γ_2^L, and γ_3^L and the new valence band parameters γ_1, γ_2, and γ_3 are given by

$$\gamma_1 = \gamma_1^L - \left(-\frac{1}{3}F\right) \quad \gamma_2 = \gamma_2^L - \left(-\frac{1}{6}F\right) \quad \gamma_3 = \gamma_3^L - \left(-\frac{1}{6}F\right)$$

and then we obtain $\mathcal{E}_G = \mathcal{E}_c - \mathcal{E}_v$ and the spin–orbit splitting Δ_0

$$\begin{aligned}
\gamma_1 &= \gamma_1^L - \frac{1}{3}\cdot\frac{\mathcal{E}_P}{3}\left[\frac{2}{\mathcal{E}_G} + \frac{1}{\mathcal{E}_G + \Delta_0}\right] \\
\gamma_2 &= \gamma_2^L - \frac{1}{6}\cdot\frac{\mathcal{E}_P}{3}\left[\frac{2}{\mathcal{E}_G} + \frac{1}{\mathcal{E}_G + \Delta_0}\right] \\
\gamma_3 &= \gamma_3^L - \frac{1}{6}\cdot\frac{\mathcal{E}_P}{3}\left[\frac{2}{\mathcal{E}_G} + \frac{1}{\mathcal{E}_G + \Delta_0}\right]
\end{aligned}$$

2.5(9) Valence band parameters

Table: Band parameters of Ge, Si, GaAs, InAs, AlAs, and GaP

Parameters	Ge	Si	GaAs	InAs	AlAs	GaP
$\mathcal{E}_G^{\Gamma}$ [eV]	0.8872	4.185	1.519	0.417	3.099	2.886
$\mathcal{E}_G^{X}$ [eV]	1.3	1.17	1.981	1.433	2.24	2.35
$\mathcal{E}_G^{L}$ [eV]	0.82	n.a.	1.815	1.133	2.46	2.72
Δ_0 [eV]	0.297	0.044	0.341	0.39	0.28	0.08
$m_e^*(\Gamma)$	n.a.	n.a.	0.067	0.026	0.15	0.13
$m_l^*(L)$	1.57	n. a.	1.90	0.64	1.32	2.0
$m_t^*(L)$	0.0807	0.19	0.075	0.05	0.15	0.253
$m_l^*(X)$	n.a.	0.916	1.98	1.13	0.97	1.2
$m_t^*(X)$	n.a.	0.19	0.27	0.16	0.22	0.15
γ_1	13.35	4.26	6.98	20.0	3.76	4.05
γ_2	4.25	0.38	2.06	8.5	0.82	0.49
γ_3	5.69	1.56	2.93	9.2	1.42	2.93
$\mathcal{E}_P$ [eV]	26.3	21.6	28.8	21.5	21.1	31.4
F	-27.2	-5.14	-17.8	-43.3	-6.62	-10.78
$F^{\dagger}$			(-1.94)	(-2.90)	(-0.48)	(-2.04)

2.5(10) Alignment of conduction bands

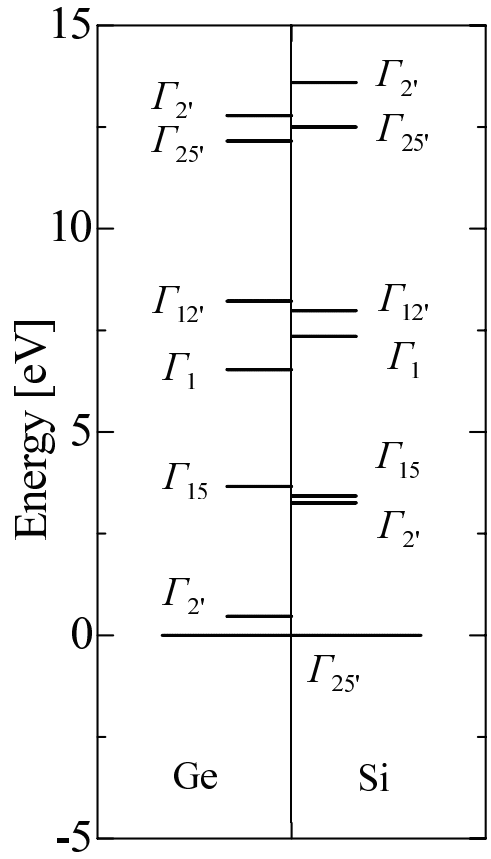

Figure: Alignment of the conduction bands for Ge and Si calculated by 15×15 empirical pseudopotential method

The speaker would like to thank the organizers for giving the chance to present this short course lecture.

If you have any questions, please feel free to contact the speaker during the workshop.

If you are interested in detailed treatments of 8×8 $\boldsymbol{k} \cdot \boldsymbol{p}$ perturbation for the case of **quantum dot superlattices** and evaluations of absorption coefficients, please visit posters:

T. Kotani, H. Yoshikawa, *et al.*; **P30**

H. Yoshikawa, T. Kotani, *et al.*: **P31**

Thank you